IEEE Access
Multidisciplinary | Rapid Review | Open Access Journal

Received September 13, 2021, accepted September 21, 2021, date of publication September 24, 2021,
date of current version October 5, 2021.

Digital Object Identifier 10.1109/ACCESS.2021.3115707

A Technique for the Early Detection of Brain Cancer Using Circularly Polarized Reconfigurable Antenna Array

DEMYANA A. SALEEB[1], REHAB M. HELMY[2], NIHAL F. F. AREED[3], MOHAMED MAREY[4], (Senior Member, IEEE), WAZIE M. ABDULKAWI[5], AND AHMED S. ELKORANY[2]

[1]Faculty of Engineering, Kafrelsheikh University, Kafr El-Shaikh 33516, Egypt
[2]Faculty of Electronic Engineering, Menoufia University, Minuf 32952, Egypt
[3]Faculty of Engineering, Mansoura University, Mansoura 35516, Egypt
[4]Smart Systems Engineering Laboratory, College of Engineering, Prince Sultan University, Riyadh 11586, Saudi Arabia
[5]Electrical Engineering Department, Faculty of Engineering, King Saud University, Riyadh 11421, Saudi Arabia

Corresponding author: Demyana A. Saleeb (demyanasaleeb@eng.kfs.edu.eg)

This work was supported by Prince Sultan University (by paying the Article Processing Charges (APC) of this publication).

ABSTRACT In this paper, a technique for the early detection of brain cancer was proposed. The technique depends upon the use of an antenna and a model for the human head. The reflection coefficient (S_{11}) was found for two cases: with and without tumor in the head model. The large increase of S_{11} due to the presence of the tumor provides a good indication for tumor detection. It also gives an idea about the size of the tumor. The antenna used was a reconfigurable four-element linear array of squared microstrip patches. Two arrays were designed one circularly polarized, the other linearly polarized. The antenna operates at Industrial Scientific and Medical (ISM) frequency 2.4 GHz. It was designed on FR-4 (lossy) substrate of relative permittivity 4.3 and thickness of 1.6 mm. To feed the array, a corporate feeding network was designed. The reconfigurability of the array was achieved using three single pole double throw (SPDT) switches. Two models of the human head were used; a specific anthropomorphic mannequin (SAM) model, and a 3-D head model consisting of four different head layers: skin, fat, skull and brain. The simulation calculates the reflection coefficient (S_{11}) with and without tumor for circularly polarized (CP) and linearly polarized (LP) linear array. Calculations were taken for four sizes of the array. The best results were obtained with the four-element circularly polarized array. An increase in S_{11} of 1188% was obtained. Tumors as small as 5 millimeters (four-layer model) and 2.5 mm (SAM model) can be detected. Specific absorption rate (SAR) was calculated and found to be within the safe limit. A circularly polarized four-element linear antenna array was fabricated. The measured S_{11} and radiation pattern are in excellent agreement with simulated ones.

INDEX TERMS Antenna arrays, brain cancer tumors, circular polarization, reconfigurable antenna, S_{11}.

I. INTRODUCTION

There is no doubt that, cancer is considered as one of the most serious diseases. It is the growth of abnormal cells in human body. According to the National Cancer Institute, there are over 100 types of cancer [1], [2].

Brain cancer is one of the most dangerous types of cancers. This is because brain is the most critical and complex organ of the human body, as it controls the nerves leading to all other organs. Brain tumours are categorized as primary or secondary. A primary brain tumour originates in the brain. A secondary brain tumour, occurs when cancer cells spread to brain from another organ, such as lung or breast [3]. Brain tumor is diagnosed by several methods such as skull x-rays, biopsy, computer tomography (CT) or magnetic resonance imaging (MRI) on head [4]. Recently, microwave tomography and radar-based imaging techniques are other ways to detect and diagnose tumors. These are low cost, and portable methods. The difference in the dielectric properties between healthy and non-healthy brain tissues is the basis for diagnosis in microwave systems [5]–[7].

The main purpose of this paper is to present a technique for the early detection of brain cancer. A reconfigurable circularly polarized patch antenna array which is simple, low

The associate editor coordinating the review of this manuscript and approving it for publication was Mohammad Zia Ur Rahman.

cost and efficient was designed. Detection of the tumor is based upon measurement of S_{11} due to single, double, triple and quadruple antenna elements. This is accomplished by using three SPDT switches [8]. Two models of the head were used; SAM model and a model consists of four layers; skin, fat, skull, and brain [9]. S_{11} was computed for two cases: with and without tumor. The difference between them was used for the detection of the tumor. Tumors tissues have higher dielectric constant compared to normal tissues. The specific absorption rate (SAR) was computed and found to be less than the safety level [10], [11].

A circularly polarized four-element linear antenna array was fabricated. The measured S_{11} and radiation pattern are in excellent agreement with simulated ones. Simulations were carried out using both finite element and finite integral techniques.

The paper is organized as follows. Section 2 includes design of the proposed antenna, design of the corporate feeding network, description of the SPDT switch, the fabricated antenna and the measured S_{11} and radiation pattern. In Section 3 simulation results of circularly polarized and linearly polarized arrays are presented. The difference in reflection coefficient (ΔS_{11}) between the two cases: with and without tumor is given. The results due to the SAM model are given in section 4. Section 5 includes the calculated values of SAR. Finally, in section 6 the conclusions are presented.

II. PROPOSED DESIGN

A. ANTENNA GEOMETRY

The CP reconfigurable patch antenna array on a head phantom for brain tumour detection is shown in Fig. 1. The squared patch antenna is designed on FR4-substrate with relative permittivity (ε_r) = 4.3 and thickness 1.6 mm with loss tangent (δ) = 0.025. The dimensions of the array are 200mm × 78mm. The substrate is above a rectangular metallic ground plane with thickness 0.035mm. The side length of the square patch is 30 mm. The antenna is fed by a corporate feed network. When the corners of the patch are truncated [17]–[19] the antenna radiates circularly polarized wave. The truncated part is a right isosceles triangle with side 5mm.

B. FEEDING NETWORK

The corporate feed network and antenna patches are drawn in Fig.1. The input impedance of each patch [20] is given by:

$$Z_{in} = \frac{1}{2G_e} \tag{1}$$

and,

$$G_e = \frac{W_1}{120\lambda_0} \tag{2}$$

where, W_1 is the side length of the squared patch (30 mm), and $\boldsymbol{\lambda_0}$ is the free space wave length equals 125 mm corresponding to the resonance frequency 2.4 GHz.

Refer to "(1)," the input impedance of the patch equals 250 Ω. The quarter wave length transformer T_1 matches

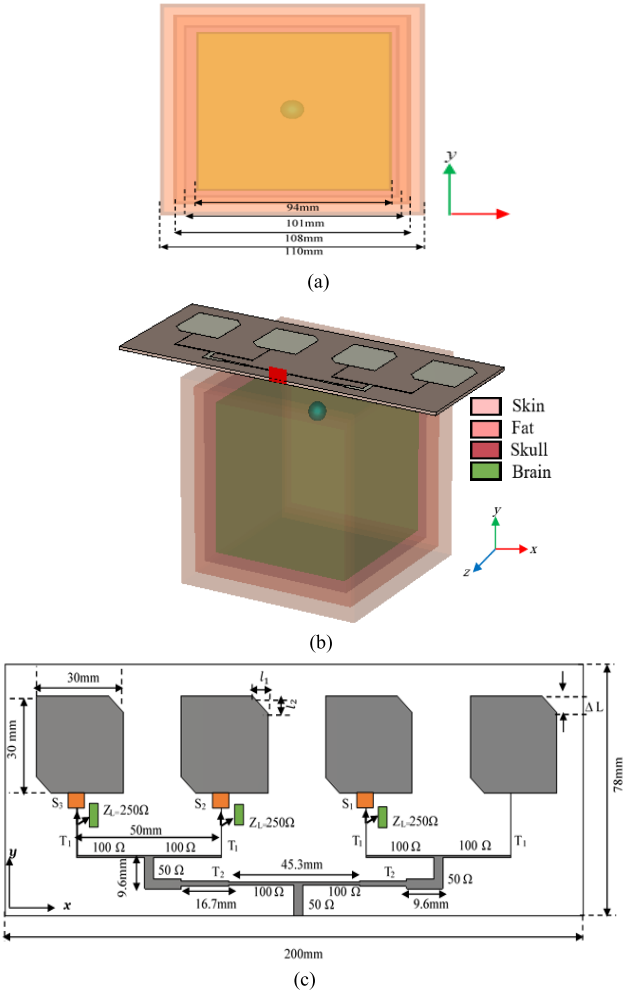

FIGURE 1. Geometrical structure of proposed antenna (a) 3-D side view of head phantom, (b) top view of the human head model with tumor, (c) top view of the antenna array structure with switches.

the patch to 100 Ω. The characteristic impedance [21] is obtained by:

$$Z_{T_1} = \sqrt{Z_{in} * Z_{out}} = \sqrt{100 * 250} = 158\ \Omega. \tag{3}$$

where, Z_{in} is the characteristic impedance of the transmission line and Z_{out} is the input impedance of the patch at resonance.

The characteristic impedance of the quarter wave length transformer T_2 which connects the 100 Ω and 50 Ω transmission lines is

$$Z_{T_2} = \sqrt{50 * 100} = 70.7\ \Omega \tag{4}$$

The width (W_2) of the transmission line with characteristic impedance (Z_o) is given by [22]:

$$\frac{W_2}{h} = \frac{2}{\pi}B - 1 - \ln(2B-1) + \frac{\epsilon_r - 1}{2\epsilon_r}\left[\ln(B-1) + 0.39 - \frac{0.61}{\epsilon_r}\right], \quad for\ A > 1.52 \tag{5}$$

TABLE 1. The width of the feed lines of 158Ω, 100Ω, 70Ω, and 50Ω.

Input impedance (Ω)	Line width (mm)
158	0.14
100	0.65
70.7	1.1
50	3.11

where,

$$A = \frac{Z_0}{60}\{\frac{\epsilon_r + 1}{2}\}^{-1/2} + \frac{\epsilon_r - 1}{\epsilon_r + 1}0.23 + \frac{0.11}{\epsilon_r} \quad (6)$$

and

$$B = \frac{60\pi^2}{Z_0\sqrt{\epsilon_r}} \quad (7)$$

The lengths of the transmission lines can be found from [24]:

$$l = \frac{\lambda}{4\sqrt{\epsilon_{r_{eff}}}} \quad (8)$$

where,

$$\epsilon_{r_{eff}} = \frac{\epsilon_r + 1}{2} + \frac{\epsilon_r - 1}{2}[1 + \frac{12h}{W_1}]^{-1/2} \quad (9)$$

The widths of the transmission lines at 50Ω, 70.7Ω, 100 Ω, and 158 Ω input impedance are shown in Table 1.

The input impedance of the antenna array and corporate feed network was computed. Simulations were carried out using CST and HFSS simulations tools. Fig. 2(a) shows the real part of the input impedance which is 50 Ω at the design frequency 2.4 GHz. The imaginary part of the impedance is shown in Fig.2 (b) which is zero at the operating frequency, so perfect matching is achieved. Additionally, three single pole double throw switches (SPDT) S_1, S_2, and S_3 are used to reconfigure the antenna array. The number of operating patches of the array is controlled by the switches. The circuit diagram of the (SPDT) is illustrated in Fig. 3, D_1 and D_2 are PIN diodes. To link ports 1 and 2, D_1 must be OFF and D_2 ON. Thus, when D_2 is ON (short circuit) the input impedance to the $\lambda/4$ line will be open preventing signal from reaching port 3. Similarly; to connect ports 1 and 3, D_2 is OFF and D_1 is ON. Therefore, in the corporate feeding network port 2 represents the patch and port 3 is set to 250 Ω to replace the input impedance of the patch.

The switches cause a small shift in resonance frequency. They also cause small loss in power which affects efficiency.

The head phantom contains four layers skin, fat, skull, and brain with side lengths 110mm, 108 mm, 101 and 94 mm respectively [9], [27]. The cancerous tumor is considered spherical with relative permittivity 70 and electric conductivity 2.3 [24], [25]. The dielectric properties of human model tissues are illustrated in Table. II.

The axial ratio is shown in Fig.4. It can be shown from this figure that the axial ratio obtained by CST simulation is

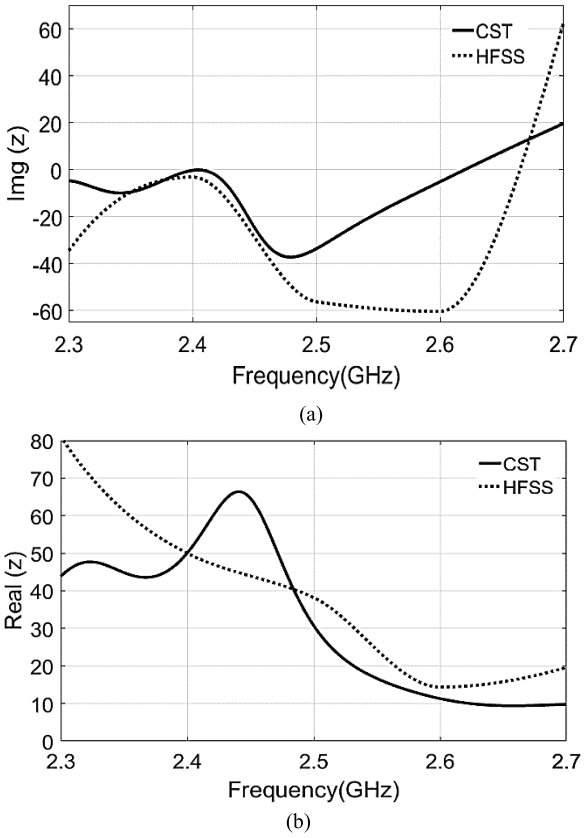

FIGURE 2. The input impedance of the antenna array and corporate feed network, (a) Z(real), (b) Z(img).

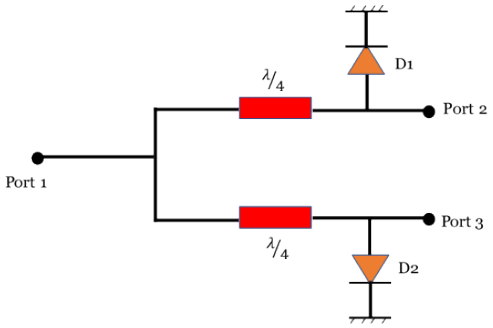

FIGURE 3. Circuit diagram of the SPDT switch.

TABLE 2. The electrical properties of the phantom model of human brain.

Tissue	Brain	Skull	Fat	Skin	Tumor
Relative permittivity	49.7	17.8	10.8	46.7	70
Conductivity S/m	0.59	0.16	0.28	0.69	2.3

0.8 dB at the resonance frequency 2.4 GHz with 1.7 % of B.W below 3 dB. A good agreement between CST and HFSS can be observed.

C. EXPERIMENTAL

The full size (four-element) array gave a large increase of S_{11} of 1188%. Therefor it was decided to fabricate this array.

TABLE 3. Δ S_{11} for Cp and Lp.

	Single element	2- elements	3- elements	4- elements
CP without tumor	-17.3 dB	-30.45dB	-41.71dB	-49.5dB
CP with tumor	-14.2dB	-19.86dB	-24.3dB	-28 dB
Δ S with CP	3.1dB	10.58dB	17.41dB	21.5dB
LP without tumor	-10. 6dB	-21.6dB	-19.7dB	-29 dB
LP with tumor	-9.8dB	-19.3dB	-16.3 dB	-24.5 dB
Δ S with LP	0.8 dB	2.3dB	3.4dB	4.5 dB
% Increase	287.5%	360%	412%	377.78%

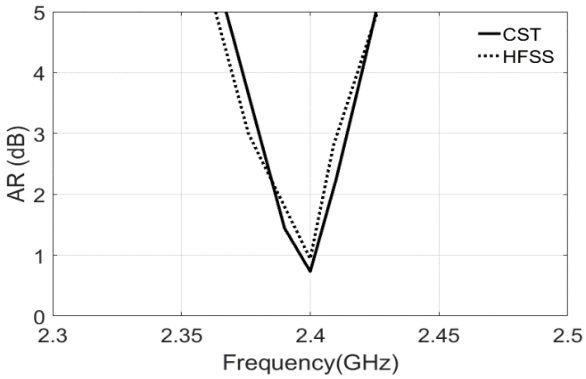

FIGURE 4. Axial ratio of the antenna array.

TABLE 4. Δ S and the shift in resonance frequency for each stage of tumor (Sam model).

Stage	S_{11} (dB)	ΔF (MHz)	ΔS (dB)
No tumor	-31	-	-
Tumor radius 2.5mm	-6.5	40	24.5
Tumor radius 5mm	-6.3	41	24.7
Tumor radius 10mm	-7	46	24
Tumor radius 15mm	-3	46.5	28
Tumor radius 20mm	-2.6	47.5	28.4
Tumor radius 25mm	-2.6	48.7	28.4
Tumor radius 30mm	-2.5	49	28.5
Tumor radius 35mm	-2.3	49.5	28.7

The full size array does not need switches. The fabricated array is shown in Fig. 5. The radiation pattern and S_{11} were measured in free space. Antenna measurement system of Geozondas [26] was used (Fig. 6), which is a pulse time domain measurement system. The measured and simulated S_{11} are shown in Fig. 7.

Measurement shows resonance at 3 GHz. Therefore, the simulation was extended to 4 GHz and showed resonance at 3.75 GHz. The designed antenna is intended to work at 2.4 GHz, therefore the antenna behaviour away from this frequency is out of our interest. The impedance bandwidth of the antenna is determined by taking the 10-dB bandwidth of S_{11} which is equal to 88.3 MHz in simulation and 90.9 MHz in measurement.

Moreover, the measured and simulated radiation patterns are shown in Fig.8. Very good agreement between simulation and measurement can be noticed.

III. SIMULATION RESULTS AND DISSCUSSION

A. CP ANTENNA ARRAY SIMULATION

In this subsection, the CP reconfigurable antenna array with head phantom is simulated. The changes of reflection coefficient (ΔS_{11}) is calculated to distinguish between head phantom with and without tumor as;

$$\Delta S_{11} = S_{11}(with\ tumor) - S_{11}(with\ out\ tumor) \quad (10)$$

The number of patches operating in the array is controlled by the SPDT switches. Four sizes of the array are investigated and simulated. The return loss is calculated for each array size put upon human head model with and without tumor. The results are summarized in Table 3.

B. LINEARLY POLARIZED (LP) ANTENNA ARRAY

Linear polarization is obtained when the square patches have no truncation at the corners. The resonance frequency becomes 2.3 GHz. The wave length λ_o becomes 129 mm. The input impedance of the patch Z_{in} becomes 259.5 Ω. The characteristic impedance of the quarter wave transformer T_1 changes to 161 Ω. The characteristic impedance of the quarter wave transformer T_2 stays at 70.7 Ω. Hence, the width of the quarter wave transformer T_1 can be calculated from equations (5-7) and changed to 0.138 mm. The simulation results of S_{11} for the four sizes of the array are shown in Table 3. There is a great difference between the results of the S_{11} in circular polarization and linear polarization. This means that circularly polarized array is much better than the linearly polarized array for the detection of brain tumor. Table 3. summarizes the results of S_{11} for CP and LP and the percentage increase of ΔS_{11} for CP over LP. Fig. 9 shows S_{11} with the size of the array for CP and LP. The CP arrays give a large difference in S_{11} between the two cases: with and

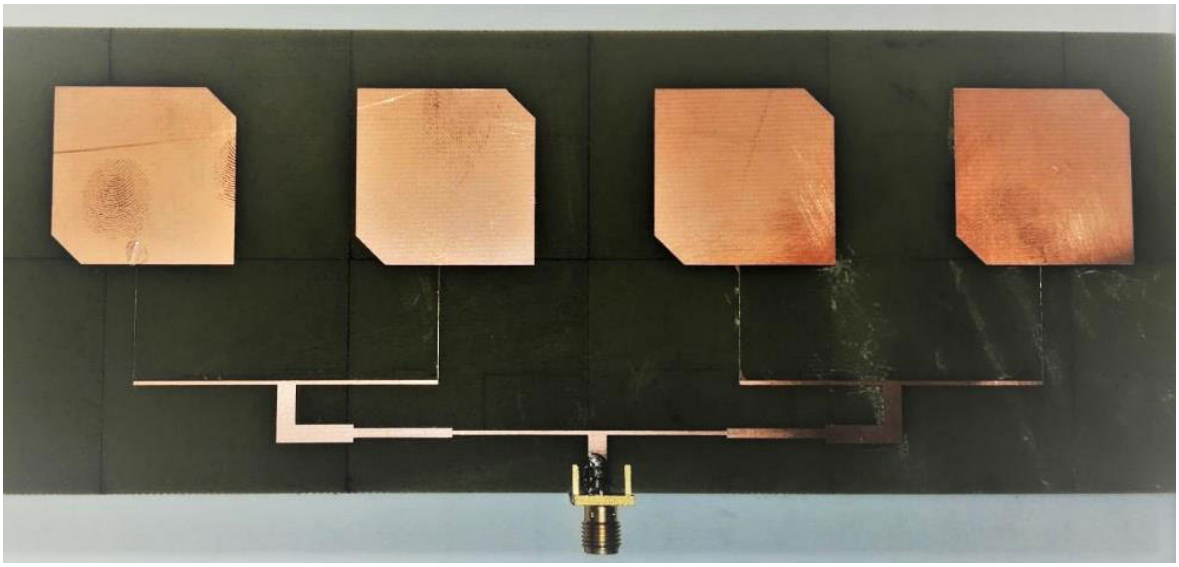

FIGURE 5. Fabricated antenna.

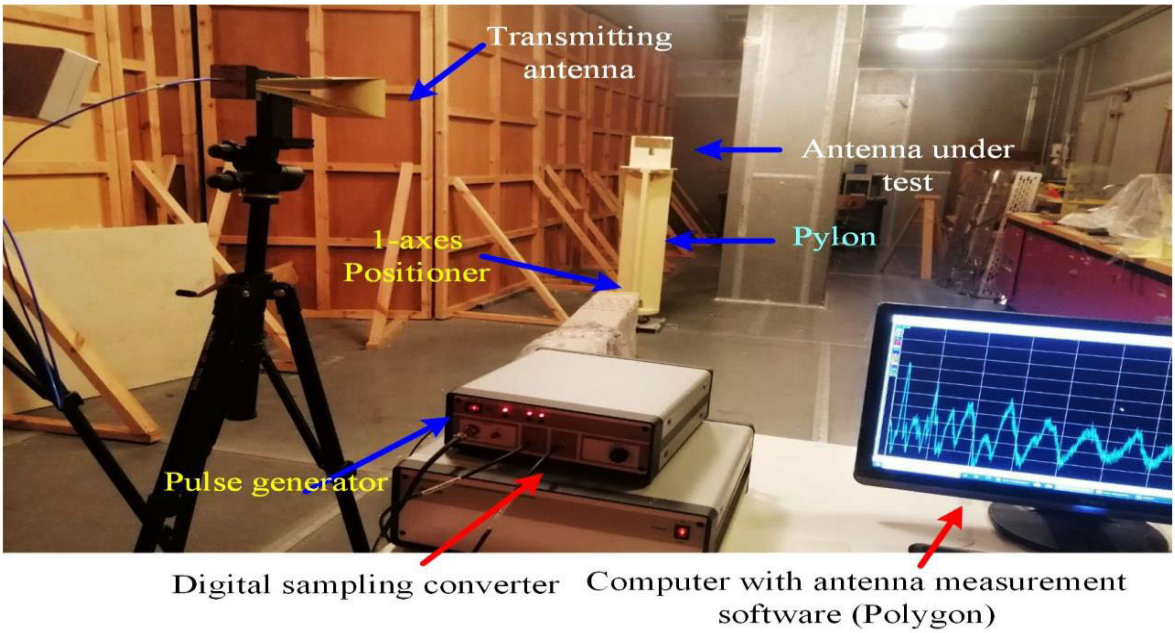

FIGURE 6. Measurement setup.

without tumor. Circular polarization gives much better results than linear polarization.

Fig. 10 shows variation of S_{11} with tumor size. Reflection increases as the tumor size increases. This enables us not only to detect the presence of tumor but also to predict the size of the tumor.

IV. VALIDATION OF THE RESULTS WITH SAM HEAD MODEL

In this section SAM head model in CST is used to find S_{11}. SAM head model and CP array are shown in Fig.10(a). The CP antenna array is put above the head model. The results of S_{11} are presented for different sizes of the tumor. The differences in the reflection coefficient ΔS and the shift in resonant frequency ΔF are summarized in Table 4. Fig. 11 (b) shows the simulated results of the reflection coefficient at each stage of tumor. It can be noted that, tumors as small as 2.5 mm can be detected.

V. SPECIFIC ABSORBITION RATE (SAR)

In this section SAR for 10 grams of tissue are computed for the head phantom with CP array. The value of SAR is important for human body safety. SAR can be calculated from the following formula [11]:

TABLE 5. Sar values for single, 2-, 3- and 4-element Cp array.

	Single element		2-elements		3-elements		4-elements	
	No tumor	tumor	No tumor	tumor	No tumor	tumor	No tumor	tumor
SAR(W/Kg)	0.09	0.0966	0.0888	0.0945	0.082	0.091	0.072	0.081
% Increase		7.33		6.42		10.97		12.5

TABLE 6. A comparison with the published research works.

Reference	Antenna configuration	Frequency band	The used technique	Results
[9]	UWB antenna single element	3.356 to 12.604 GHZ	Frequency shift (S_{11})	213 MHz shift in S_{11} between simulated head model with and without tumor.
[11]	UWB antenna array 4×1	1.6 to 10.8 GHz	SAR	SAR of brain with tumor was138.7% larger than without tumor.
[12]	Wearable pentagon microstrip patch antenna	ISM band from 2.4 - 2.4835 GHz.	S_{11}, E- field	Small Changes of S_{11} between with and without tumor at three positions: 4.86%, 0.822%, 0.61%, also, small differences in E- field 0.04%, 0.06%, 0.02%.
[13]	UWB Vivaldi Antenna	100 MHz to 1.4 GHz	S_{11}	13% increase in S_{11} between phantom with and without tumor
[14]	Rectangular microstrip patch antennas	2 - 2.483 GHz	SAR, S_{11}, E- field, H- field	The differences in S_{11}, E-field, H-field, SAR value were 118%, 5%, 79%,3.9% respectively.
[15]	Compact microstrip patch antenna with metamaterial	3 - 4.5 GHz	SAR, current density, H- field	The differences in current density, H-field, SAR value were 200%, 0.5%, 170% respectively.
[16]	UWB Rectangular microstrip patch antenna	6- 8.5 GHz	S_{11}, current density, SAR.	The increases of S_{11}, current density, and SAR are 7.76%,1.92% and 88.9% respectively.
[28]	Wearable microstrip patch antenna	around 2.6 GHz	SAR	207% increase in SAR with tumor than without tumor.
Proposed structure	4×1squared patch antenna array	ISM band from 2.4 to 2.45 GHz	S_{11}	Increase in S_{11} of 21.5 dB over the case of no tumor.

$$SAR = \frac{\sigma\,|E|^2}{\rho} \tag{11}$$

where σ is the electric conductivity of tissue (S/m), E is the electric field intensity (V/m) and ρ is tissue mass density (Kg/m^3). According to IEEE C95.1, the limit value of SAR is 2W/kg.

Table 5 records the value of SAR for the four sizes of the array. There is little increase in SAR due to the presence of the tumour and it is still below the safety level.

A comparison between published works and the current work has been introduced in Table 6.

This table shows that researches depend upon one or more of the following parameters for the detection of tumor S_{11},

SAR, current density, E-field, and H-field. Two papers refer to increase of current density of 1.92% and 0.5%.

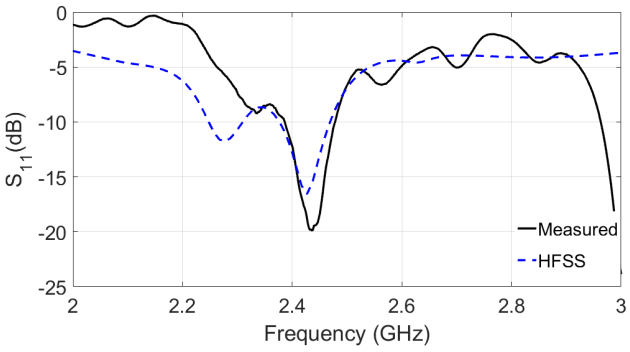

FIGURE 7. Measured and simulated S_{11}.

It is clear that the current density cannot be depended upon for tumor detection. Two papers refer to an increase of magnetic field of 170% and 3.9%. Two

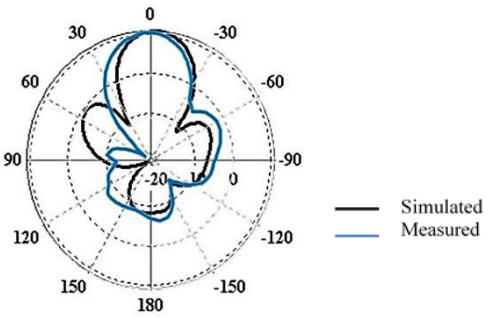

FIGURE 8. Measured and simulated radiation pattern.

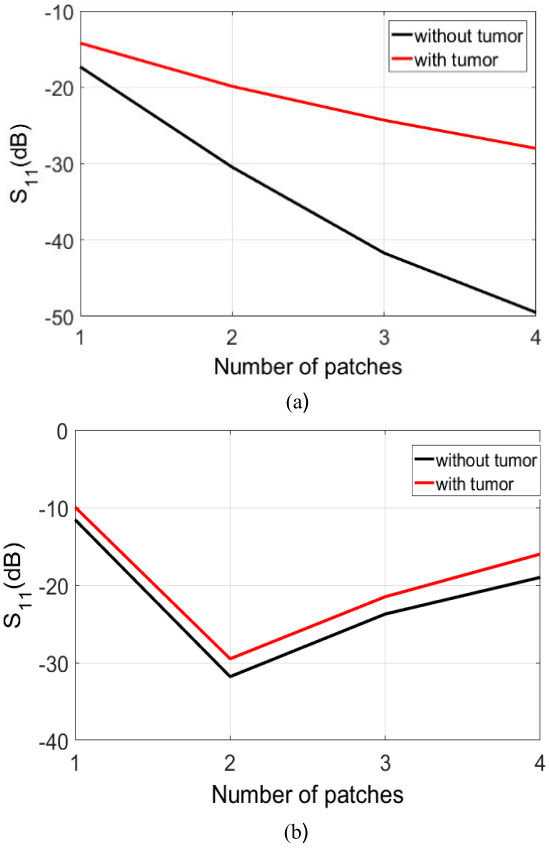

FIGURE 9. The values of S_{11} with the number of operational patches in (a) CP, (b) LP.

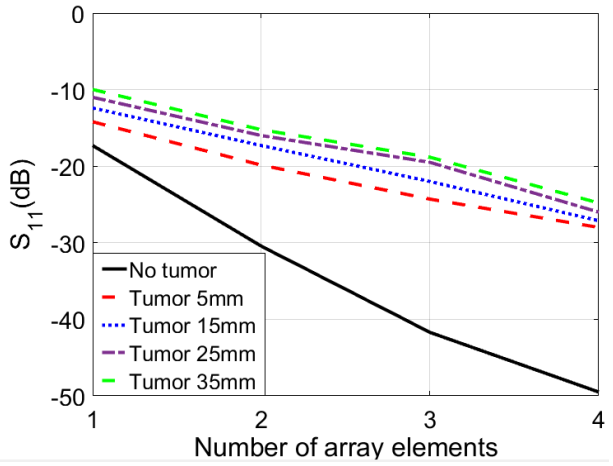

FIGURE 10. S_{11} vs. number of antenna elements with tumor size as a parameter.

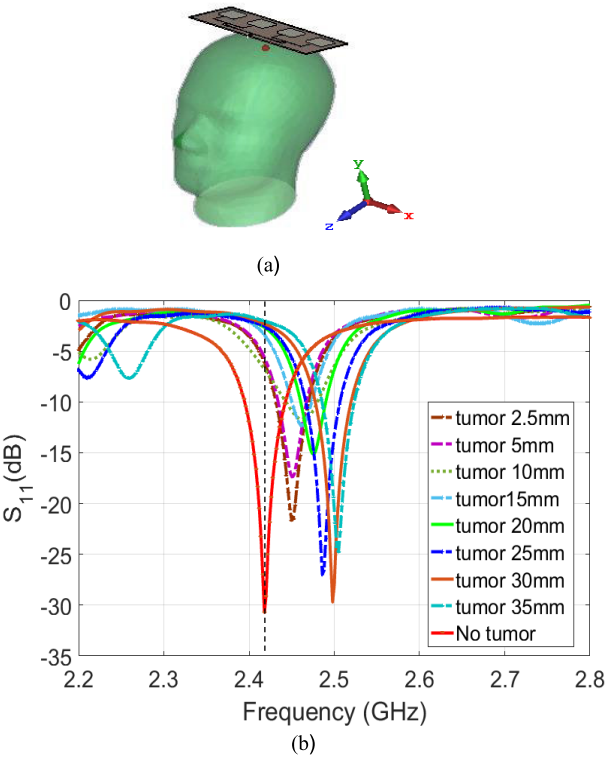

FIGURE 11. (a) SAM head model and the CP antenna array, (b) the simulated results of S_{11}.

papers refer to an increase of electric field of 79% and 0.04%.

Five papers refer to an increase in SAR of 138.7%, 118%, 200%, 88.9%, and 207%. It is not enough to mention the increase in SAR due to tumor. It is important to mention if the system is within the safe limits. Four papers refer to an increase in S_{11} of 4.86%, 13%, 118%, and 7.76%. The proposed system in this paper shows an increase 0f 21.5 dB in S_{11} which corresponds to a percentage increase of 1188%. This shows the superiority of the proposed system.

VI. CONCLUSION

A reconfigurable four-element circularly polarized linear antenna array was designed for brain tumor detction. A corporate feeding network was designed to match the antenna to the feeding source. Reconfigurability of the array was achieved using three single-pole double throw switches. The switches used PIN diodes. S_{11} was found for the antenna array on head phantom with and without tumor. S_{11} was found for four sizes of the array. The difference ΔS_{11} between the two cases; with

and without tumor was found to be 3.1, 10.58, 17.41, 21.5 dB. The last three values are large enough to enable detection of brain tumors. The difference ΔS_{11} enable detection of small tumors (5 mm).The SAM head model in CST was simulated and S_{11} was computed. Tumors as small as 2.5 mm can be detected. This enables early detection of brain cancer.

A four-element linearly polarized linear array was designed and ΔS_{11} was found. ΔS_{11} for circular polarization was found to be larger than that for linear polarization by 377.78%, 412%, 360%, and 287.5% for the four sizes of the array. Circular polarization gives much better results. The values of SAR were calculated for the four sizes of the array and were found to be 0.097, 0.095, 0.091, and 0.081 W/Kg. These values are below the safe limit of exposure (2 W/Kg).

The four-element circularly polarized linear antenna array, but without the SPDT switches, was fabricated. The radiation pattern and S_{11} were measured in free space. Very good agreement between simulation and measurement was noticed.

REFERENCES

[1] K. D. Miller, L. Nogueira, A. B. Mariotto, J. H. Rowland, K. R. Yabroff, C. M. Alfano, A. Jemal, J. L. Kramer, and R. L. Siegel, "Cancer treatment and survivorship statistics," *CA, Cancer J. Clinicians*, vol. 69, no. 5, pp. 363–385, 2019.

[2] R. Capuano, A. Catini, R. Paolesse, and C. Di Natale, "Sensors for lung cancer diagnosis," *J. Clin. Med.*, vol. 8, no. 2, p. 235, Feb. 2019.

[3] B. W. Pope, "Brain metastases: Neuroimaging," in *Handbook of Clinical Neurology*, vol. 149. Amsterdam, The Netherlands: Elsevier, 2018, pp. 89–112.

[4] S. A. K. Al-Nahiun, F. Mahbub, R. Islam, S. B. Akash, R. R. Hasan, and M. A. Rahman, "Performance analysis of microstrip patch antenna for the diagnosis of brain cancer & tumor using the fifth-generation frequency band," in *Proc. IEEE Int. IoT, Electron. Mechatronics Conf. (IEMTRONICS)*, Apr. 2021, pp. 1–6.

[5] R. Inum, M. M. Rana, K. N. Shushama, and M. A. Quader, "EBG based microstrip patch antenna for brain tumor detection via scattering parameters in microwave imaging system," *Int. J. Biomed. Imag.*, vol. 2018, pp. 1–12, Feb. 2018.

[6] E. R. Alagee and A. Assalem, "Brain cancer detection using U-shaped slot Vivaldi antenna and confocal radar-based microwave imaging algorithm," *Amer. Sci. Res. J. Eng., Technol., Sci.*, vol. 66, no. 1, pp. 1–13, 2020.

[7] T. Singh, S. Singh, M. Singh, and R. Kaur, "Design of patch antenna to detect brain tumor," in *Proc. Int. Conf. Issues Challenges Intell. Comput. Techn. (ICICT)*, Sep. 2019, pp. 1–6.

[8] N. A. Shairi, Z. Zakaria, A. M. S. Zobilah, B. H. Ahmad, and P. W. Wong, "Design of SPDT switch with transmission line stub resonator for WIMAX and LTE in 3.5 GHz band," *ARPN J. Eng. Appl. Sci.*, vol. 11, no. 5, pp. 3198–3202, Mach 2016.

[9] M. A. Shokry and A. M. M. A. Allam, "UWB antenna for brain stroke and brain tumor detection," in *Proc. 21st Int. Conf. Microw., Radar Wireless Commun. (MIKONN)*, Krakow, Poland, May 2016, pp. 1–3.

[10] P. J. Soh, G. Vandenbosch, F. H. Wee, A. van den Bosch, M. Martinez-Vazquez, and D. Schreurs, "Specific absorption rate (SAR) evaluation of textile antennas," *IEEE Antennas Propag. Mag.*, vol. 57, no. 2, pp. 229–240, Apr. 2015.

[11] M. A. Jamlos, W. A. Mustafa, W. Khairunizam, I. Zunaidi, Z. M. Razlan, and A. B. Shahriman, "Tumor detection via specific absorption rate technique using ultra-wideband antenna," *IOP Conf. Ser., Mater. Sci. Eng.*, vol. 557, Jun. 2019, Art. no. 012024.

[12] R. Raihan, M. S. A. Bhuiyan, R. R. Hasan, T. Chowdhury, and R. Farhin, "A wearable microstrip patch antenna for detecting brain cancer," in *Proc. IEEE 2nd Int. Conf. Signal Image Process. (ICSIP)*, Aug. 2017, pp. 432–436.

[13] M. A. Alzabidi, M. A. Aldhaeebi, and I. Elshafiey, "Optimization of UWB Vivaldi antenna for tumor detection," in *Proc. 1st Int. Conf. Artif. Intell., Modeling Simulation*, Kota Kinabalu, Malaysia, Dec. 2013, pp. 71–76.

[14] M. J. Dishali, K. M. Kumar, and S. M. Nawaz, "Design of microstrip patch antenna for brain cancer detection," *ICTACT J. Microelectron.*, vol. 5, no. 1, pp. 731–737, Apr. 2019.

[15] H. Angelin and K. M. Kumar, "Brain tumor detection using metamaterial based microstrip patch antenna," *Int. Res. J. Eng. Technol.*, vol. 4, no. 4, pp. 3340–3344, Apr. 2017.

[16] H. K. Gupta, R. Sharma, and V. V. Thakre, "Tumor detection in multilayer brain phantom model by symmetrical-shaped DGS rectangular microstrip patch antenna," in *Proc. Int. Conf. Intell. Comput. Smart Commun.* Singapore: Springer, 2020, pp. 705–712.

[17] Z. Muludi and B. Aswoyo, "Truncated microstrip square patch array antenna 2 × 2 elements with circular polarization for S-band microwave frequency," in *Proc. Int. Electron. Symp. Eng. Technol. Appl. (IES-ETA)*, Sep. 2017, pp. 87–92.

[18] A. Chrysler, C. Furse, R. N. Simons, and F. A. Miranda, "A Ka-band (26 GHz) circularly polarized 2×2 microstrip patch sub-array with compact feed," in *Proc. IEEE Int. Symp. Antennas Propag., USNC/URSI Nat. Radio Sci. Meeting*, Jul. 2017, pp. 1447–1448.

[19] G. S. Kirov, "Evaluation of the frequency bandwidth and gain properties of antennas: Characteristics of circularly polarized microstrip antennas," *IEEE Antennas Propag. Mag.*, vol. 62, no. 3, pp. 74–82, Jun. 2020.

[20] N. Ab Wahab, Z. B. Maslan, W. N. W. Muhamad, and N. Hamzah, "Microstrip rectangular 4×1 patch array antenna at 2.5 GHz for WIMAX application," in *Proc. 2nd Int. Conf. Comput. Intell., Commun. Syst. Netw.*, 2010, pp. 164–168.

[21] R. Bancroft, *Microstrip and Printed Antenna Design*, 3rd ed. London, U.K.: The Institution of Engineering and Technology, 2019, ch. 2, sec. 1, pp. 26–31.

[22] A. Balanis, *Antenna Theory: Analysis and Design*, 3th ed. Hoboken, NJ, USA: Wiley, Dec. 2015, ch. 14, sec. 2, pp. 820–825.

[23] S. Sharma, C. C. Tripathi, and R. Rishi, "Impedance matching techniques for microstrip patch antenna," *Indian J. Sci. Technol.*, vol. 10, no. 28, pp. 1–16, 2017.

[24] S. Gabriel, R. W. Lau, and C. Gabriel, "The dielectric properties of biological tissues: II. Measurements in the frequency range 10 Hz to 20 GHz," *Phys. Med. Biol.*, vol. 41, no. 11, pp. 2251–2269, Nov. 1996.

[25] K. R. Foster and J. L. Schepps, "Dielectric properties of tumor and normal tissues at radio through microwave frequencies," *J. Microw. Power*, vol. 16, no. 2, pp. 107–119, Jan. 1981.

[26] Geozandas.com. *Time Domain Antenna Measurement Systems*. [Online]. Available: https://www.geozondas.com/main_page.php?pusl=12

[27] A. S. Elkorany, R. M. Helmy, A. A. Saleeb, and N. F. Areed, "Microstrip patch antenna linear arrays for brain tumor detection," in *Proc. 14th Int. Conf. Comput. Eng. Syst. (ICCES)*, Cairo, Egypt, Dec. 2019, pp. 425–431.

[28] Suriya, R. Nandhini, M. Leepika, and S. R. Praveen, "Microstrip patch antenna for brain tumor detection," *Int. J. Sci. Res. Rev.*, vol. 7, no. 3, pp. 63–66, 2018.

DEMYANA A. SALEEB received the B.Sc. degree (Hons.) in electronics and communication engineering from Modern Science and Arts (MSA) University, Egypt, and the M.Sc. degree in electronics and communications engineering and the Ph.D. degree in applications of electromagnetic band gap (EBG) materials for the enhancement of antennas properties from the Faculty of Electronic Engineering, Minuf, Egypt. Her thesis was on "Transmission Line Modeling Method and Applications to Antennas." She is currently a Lecturer with the Department of Physics and Engineering Mathematics, Faculty of Engineering, Kafrelsheikh University, Egypt. Her research interests include EBG materials, computational electromagnetics, and energy harvesting. She is a member of Engineering Syndicate, Egypt, and the Institution of Engineering and Technology (IET), U.K.

REHAB M. HELMY received the B.Sc. degree in electronics and communications from the Department of Electronics and Communications Engineering, Faculty of Engineering, Mansoura University, and the M.Sc. degree from Mansoura University, in 2015. Currently, she is pursuing the Ph.D. degree in communication engineering with the Faculty of Electronic Engineering, Menoufia University, Minuf, Egypt. Her thesis was on "Applications of Electromagnetic Band Gap Structures in Antenna." Her research interests include biomedical engineering and microwave applications.

NIHAL F. F. AREED received the B.Sc. degree (Hons.) in electronics and communications from the Electronic and Communication Department, Faculty of Engineering, Mansoura University, in May 2000, and the M.Sc. and Ph.D. degrees in electrical communications from the Faculty of Engineering, Mansoura University, in 2003 and 2008, respectively. In January 2001, she was appointed as a Demonstrator of the Electronic and Communication Department, Mansoura University. She was appointed as a Lecturer, in April 2008, an Associate Professor, in September 2013, and finally a Professor, in September 2018. Her research interests include microwave and antenna, optical fibers, and plasmonic models. She is a member of the IEEE Communication Society and OSA. She won the title Ideal Student of the Faculty of Engineering, in 1999. She was awarded the Scientific Excellence Award by the Egyptian Society of Engineers, in 2001. She won the State Incentive Award from the Academy of Scientific Research, in July 2018.

MOHAMED MAREY (Senior Member, IEEE) received the M.Sc. degree in electrical engineering from Menoufia University, Egypt, in 1999, and the Ph.D. degree in electrical engineering from Ghent University, Belgium, in 2008. From 2009 to 2014, he was a Research Associate and a Visiting Professor with the Faculty of Engineering and Applied Science, Memorial University, Canada. He is currently a Full Professor with the Faculty of Electronic Engineering, Menoufia University. He is on a sabbatical leave in order to join Prince Sultan University, Saudi Arabia, as the Research Laboratory Leader of the Smart Systems Engineering Laboratory. He authored the book *Multi-Carrier Receivers in the Presence of Interference: Overlay Systems* (VDM Publishing House Ltd., 2009) and around 100 scientific papers published in international journals and conferences. His main research interests include wireless communications and digital signal processing, with a particular focus on smart antennas, cooperative communications, signal classification for cognitive radio systems, synchronization and channel estimation, multiple-input multiple-output antenna systems, multicarrier systems, and error correcting codes. He was a recipient of the Young Scientist Award from the International Union of Radio Science, in 1999. He serves as an Editor for the IEEE Open Journal of the Communications Society.

WAZIE M. ABDULKAWI received the B.Sc. degree in electronics engineering from IBB University, Ibb, Yemen, in 2007, and the M.S. and Ph.D. degrees in electrical engineering from King Saud University, Riyadh, Saudi Arabia, in 2013 and 2020, respectively.

He is currently working as a Researcher with the Electrical Engineering Department, King Saud University. He has published more than 20 international publications and holds a patent for chipless RFID tags. His research interests include reconfigurable antennas, chipless RFID tags, biomedical engineering systems, and RFID sensor.

AHMED S. ELKORANY received the B.Sc. degree (Hons.) in electronics and electrical communications and the M.Sc. and Ph.D. degrees in electrical communications (microwaves and antennas) from the Department of Electronics and Electrical Communication Engineering, Faculty of Electronic Engineering, Menoufia University, in 2003, 2007, and 2011, respectively. He was appointed as a Demonstrator, in December 2003. In December 2011, he was appointed as a Lecturer and later as an Associate Professor of the Department of Electronics and Electrical Communication Engineering, Menoufia University, in August 2018. His research interests include numerical techniques, CAD tools, programming languages, UWB antennas and systems, EBG structures, wireless sensor networks and cognitive radio, metamaterials, the IoT, mobile antennas, and image processing.